

Nanoscale Transformations in Covellite (CuS) Nanocrystals in the Presence of Divalent Metal Cations in a Mild Reducing Environment

Yi Xie,[†] Giovanni Bertoni,^{†,‡} Andreas Riedinger,^{†,§} Ayyappan Sathyam,[†] Mirko Prato,[†] Sergio Marras,[†] Renyong Tu,[†] Teresa Pellegrino,[†] and Liberato Manna^{*†}

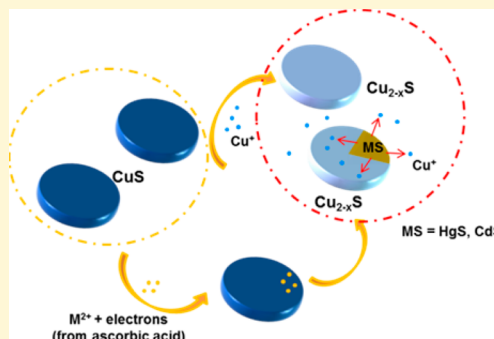
[†]Istituto Italiano di Tecnologia (IIT), via Morego, 30, 16163 Genova, Italy

[‡]IMEM-CNR, Parco Area delle Scienze 37/A, 43124 Parma, Italy

[§]Optical Materials Engineering Laboratory, ETH Zurich, 8092 Zurich, Switzerland

Supporting Information

ABSTRACT: We studied the structural and compositional transformations of colloidal covellite (CuS) nanocrystals (and of djurleite ($\text{Cu}_{1.94}\text{S}$) nanocrystals as a control) when exposed to divalent cations, as Cd^{2+} and Hg^{2+} , at room temperature in organic solvents. All the experiments were run in the absence of phosphines, which are a necessary ingredient for cation exchange reactions involving copper chalcogenides, as they strongly bind to the expelled Cu^+ ions. Under these experimental conditions, no remarkable reactivity was indeed seen for both CuS and $\text{Cu}_{1.94}\text{S}$ nanocrystals. On the other hand, in the covellite structure 2/3 of sulfur atoms form covalent S–S bonds. This peculiarity suggests that the combined presence of electron donors and of foreign metal cations can trigger the entry of both electrons and cations in the covellite lattice, causing reorganization of the anion framework due to the rupture of the S–S bonds. In $\text{Cu}_{1.94}\text{S}$, which lacks S–S bonds, this mechanism should not be accessible. This hypothesis was proven by the experimental evidence that adding ascorbic acid increased the fraction of metal ions incorporated in the covellite nanocrystals, while it had no noticeable effect on the $\text{Cu}_{1.94}\text{S}$ ones. Once inside the covellite particles, Cd^{2+} and Hg^{2+} cations engaged in exchange reactions, pushing the expelled Cu^+ ions toward the not-yet exchanged regions in the same particles, or out to the solution, from where they could be recaptured by other covellite nanoparticles/domains. Because no good solvating agent for Cu ions was present in solution, they essentially remained in the nanocrystals.



In recent years, there has been growing interest in colloidal nanocrystals (NCs) of copper chalcogenides, mainly because of their tunable near-infrared (NIR) plasmonic properties,^{1–22} and consequently their potential applications as alternatives to noble metal nanoparticles, for example in photothermal therapy for biomedicine or in sensing.^{23–32} Copper chalcogenide NC have also been investigated extensively in cation exchange (CE) reactions. In CE, the cation sublattice is partially or completely replaced by a sublattice of new types of cations, with (in principle) minor modification of the anion sublattice.^{33–37} CE reactions are regulated by various factors, such as the relative stabilities of the initial and final NC phases, as well as valency, ionic radius, and solvation energy of the entering and exiting cations.^{38–41} Solvation energies are important terms in the overall energy balance in CE: in all reported exchange reactions involving copper chalcogenide NCs, the use of phosphines (such as tributylphosphine or trioctylphosphine) is critical in order to achieve extraction of Cu^+ ions from the NCs, as these molecules are soft Lewis bases and have strong affinity with soft Lewis acids (the Cu^+ ions in this case).

In this work, we investigated the conditions under which copper chalcogenide NCs, in the specific case CuS (covellite) NCs (and $\text{Cu}_{1.94}\text{S}$ (djurleite) NCs as a control), could engage

in reactions with metal cations, in the absence of phosphines. Covellite is a structure in which the S ions have on average -1 oxidation state, due to the presence of S–S covalent bonds. This is markedly different from the most common -2 state for sulfur in the vast majority of ionic compounds involving sulfur and one or more metal cations, including $\text{Cu}_{1.94}\text{S}$.⁴² We explored whether the possibility to break these S–S bonds in covellite (by the intake of electrons from a reducing agent) could act as a driving force for the concomitant entry of metal cations in the NCs, a mechanism that would not be possible for $\text{Cu}_{1.94}\text{S}$. We chose Hg^{2+} and Cd^{2+} as test cations, based on the fact that Hg^{2+} and Cd^{2+} are classical cases of ions that, in the presence of phosphines, can be engaged in quantitative CE reactions with Cu_{2-x}S NCs.^{43–45}

In all tests, carried out at room temperature for 24 h, we found that, if the particles (both $\text{Cu}_{1.94}\text{S}$ and CuS NCs) were simply mixed with solutions of the Hg^{2+} or Cd^{2+} cations (at a metal to Cu feed ratio equal to 1:1), with no reducing agent

Received: October 5, 2015

Revised: October 15, 2015

Published: October 29, 2015



added, they exhibited a limited reactivity toward the cations, with a fraction of incorporated metal cations around 1–7% with respect to the total amount of Cu present in the NCs (Table 1).

Table 1. M:Cu Ratio (M = Cd, Hg), as Determined by ICP Analysis, in the NC Samples Collected after Reacting Covellite CuS NCs with Cd²⁺ and Hg²⁺ Cations (for 24 h), Either in the Presence or in the Absence of Ascorbic Acid

cation	M:Cu ratio (no ascorbic acid)	M:Cu ratio (with ascorbic acid)
Cd ²⁺	0.01:1	0.22:1
Hg ²⁺	0.05:1	0.20:1

Supporting Information Table S2). Then, in the presence of ascorbic acid acting as a mild reducing agent, the reactivity of covellite NCs significantly increased, with the incorporation fraction being around 20–22% (relative to Cu) and reaching values over 30% in the presence of a large excess of metal cations (in the case of Hg²⁺, a large excess of cations induced the concomitant formation of CuHgSBr). At the same time, sizes and shapes of the initial particles were essentially preserved during the reaction. On the other hand, the addition of ascorbic acid to Cu_{1.94}S NCs did not boost their reactivity toward Cd²⁺ or Hg²⁺ cations any further. These results suggest that the possibility for covellite NCs to be reduced is the main drive for their increased reactivity toward the metal cations.

We also studied in detail the structural and compositional evolution of the covellite NCs in the two cases. The reaction of Cd²⁺ and Hg²⁺ with CuS NCs led to mixtures of NCs of mainly three types: (i) NC heterostructures made of local domains of CdS (HgS) and domains of Cu_{2-x}S ($0 < x < 1$) composition; (ii) totally exchanged CdS (HgS) NCs; and (iii) NCs with Cu_{2-x}S composition. The Cu_{2-x}S NCs/domains often embedded a fraction of Cd²⁺ (Hg²⁺) ions. These reactions can be considered as being initiated by an incorporation of the metal cations in the NCs, made possible by the concomitant inflow of electrons from the reducing agent. Once in the NCs, the electrons enable the local reduction of the S anion framework via rupture of the S–S bonds, whereas the cations are locally engaged in CE reactions. Notably, the Cu⁺ ions released from the exchanged regions/NCs were not found in solution, but were rather taken up by the unexchanged covellite domains and NCs, which then acquired a Cu_{2-x}S ($0 < x < 1$) composition. Unlike the previously reported CE studies of other copper chalcogenides with Cd²⁺ and Hg²⁺, one of the notable observations in the present study is that covellite (CuS) NCs can engulf metal cations and retain copper, since a negligible release of copper species in solution is seen.

EXPERIMENTAL SECTION

Materials. Copper chloride (CuCl, anhydrous, 99.99%), copper(II) acetate monohydrate (C₄H₆CuO₄·H₂O, 99.99% trace metals basis), cadmium iodide (CdI₂, 99.990%), mercury bromide (HgBr₂, 99.9%), oleylamine (OM, >70%), and octadecene (ODE, 90%) were purchased from Sigma-Aldrich. Elemental sulfur (99%) was obtained from Strem Chemicals, and methanol (anhydrous, 99.9%) and toluene (anhydrous, 99.8%) were from Carlo Erba reagents. All chemicals were used as received without further purification.

Synthesis of Covellite NCs. Covellite CuS nanoplates were synthesized by a modified procedure previously reported by us.⁴² Briefly, a sulfur solution was prepared first by degassing a mixture of 0.160 g (5 mmol) of sulfur, 25 mL of ODE, and 25 mL of OM in a 100-mL three-neck flask at 130 °C under vacuum for 30 min. The as-formed clear yellow solution was cooled to room temperature (RT)

under N₂ atmosphere, followed by addition of 0.248 g (2.5 mmol) of CuCl and degassing at RT for an additional 60 min. The as-obtained dark green solution was then heated to 200 °C with a ramp of 8 °C/min, and it was then kept at this temperature for an additional 30 min, after which it was cooled to RT. To precipitate the NCs, methanol was added, and followed by centrifugation. The precipitate was finally dispersed in toluene for further characterizations and reactions.

Reaction of the As-Synthesized Covellite CuS NCs with Cd²⁺ and Hg²⁺ Cations. All these reactions were performed at RT in a N₂-filled glovebox. As a typical example of a reaction of CuS with Cd²⁺, and Cd²⁺ and ascorbic acid, 0.1 M solutions were prepared by respectively dissolving CdI₂ (0.0146 g) and ascorbic acid (0.0352 g) in methanol (0.4 mL for CdI₂ and 2 mL for ascorbic acid) at RT. Then, 0.4 mL of Cd²⁺ solution and 2 mL of ascorbic acid solution were added in a vial containing 4.0 mL of covellite NC dispersion (0.01 M in Cu⁺ ions, in toluene) under magnetic stirring. Aliquots (1.5 mL) of the NC solution were collected at different reaction times to monitor the evolution of morphologies, optical spectra, and compositions. The aliquots and the final sample collected after 24 h were precipitated by addition of 1.5 mL of methanol followed by centrifugation at 3000 rpm for 20 min. For all aliquots, the supernatant was then carefully collected for inductively coupled plasma–optical emission spectroscopy (ICP–OES) measurements, while the precipitate was dispersed in toluene for one additional cleaning cycle. The final precipitate was redispersed in toluene (0.5 mL) for subsequent characterization. The reactions with Hg²⁺ cations followed a similar procedure. The molar ratio of the guest cations (Cd²⁺ and Hg²⁺) introduced in the reaction environment over the Cu⁺ cations (from covellite CuS), that is, the feed ratio, was equal to 1:1 in all the reactions, except for the cases in which a large excess of guest cations was probed.

Transmission Electron Microscopy (TEM). Low-resolution TEM measurements were carried out on a JEOL JEM-1011 microscope operating at 100 kV. The samples were prepared by drop-casting NCs solutions on carbon-coated 200-mesh copper grids. High-resolution TEM (HRTEM) images were acquired on a JEOL JEM-2200FS microscope equipped with a Schottky gun working at 200 kV, a CEOS spherical aberration corrector in the objective lens allowing for a spatial resolution <1 Å, and an in-column Ω energy filter. The chemical composition of the NCs was determined by energy dispersive X-ray spectroscopy (EDS) performed in scanning mode (STEM) and by acquiring the spectra on a Bruker Quantax 400 system with a 60-mm XFlash 6T silicon drift detector (SDD). The quantification of the elements in the spectra was performed with the Cliff–Lorimer method. For HRTEM and STEM-EDS analyses the samples were prepared by drop-casting NC solutions onto ultrathin carbon-coated 300-mesh gold grids and inserted with a beryllium cup holder to avoid spurious copper signal.

X-ray Diffraction (XRD). XRD analysis was performed on a PANalytical Empyrean X-ray diffractometer equipped with a 1.8 kW Cu Kα ceramic X-ray tube and PIXcel^{3D} 2 × 2 area detector, and operating at 45 kV and 40 mA. The diffraction patterns were collected in air at room temperature using parallel-beam (PB) geometry and symmetric reflection mode. XRD data analysis was carried out using HighScore 4.1 software from PANalytical.

Elemental Analysis. ICP–OES was performed on an iCAP 6000 spectrometer (ThermoScientific) for quantification of elemental composition of NC samples and of the supernatant solutions. The samples were decomposed in aqua regia (HCl/HNO₃ equal to 3:1 (v/v)) overnight prior to ICP–OES measurements.

X-ray Photoelectron Spectroscopy (XPS). The samples were prepared in the glovebox by drop-casting a few microliters of NC solutions onto a graphite substrate (HOPG, ZYB quality, NTMDT), which was then transferred to the XPS setup in an ad hoc transfer vessel to avoid air exposure. Measurements were performed on a Kratos Axis Ultra DLD spectrometer, using a monochromatic Al Kα source (15 kV, 20 mA). Wide scans were acquired at an analyzer pass energy of 160 eV. High-resolution narrow scans were performed at constant pass energy of 10 eV and steps of 0.1 eV. Photoelectrons were detected at a takeoff angle of $\Phi = 0^\circ$ with respect to the surface normal. The pressure in the analysis chamber was maintained below 7

$\times 10^{-9}$ Torr for data acquisition. Data were converted to VAMAS format and processed using CasaXPS 2.3.16 software. The binding energy scale was internally referenced to the C 1s peak (BE for C–C = 285 eV).

Optical Spectroscopy. Raman spectra were recorded on a Jobin Yvon HR800 spectrometer. The NCs were deposited on silicon substrates under N₂. Data were acquired at $\lambda = 632.8$ nm with a 50 \times objective using a nominal power of 25 mW and integration time of 120 s. UV-vis-NIR extinction spectra on the NC solutions were performed on a Varian Cary 5000 UV-vis-NIR spectrophotometer in the 350–2000 nm range.

RESULTS AND DISCUSSION

The covellite structure is peculiar, since it is formed by a repetition, along the *c* axis, of a trilayer motif made of a layer of triangular CuS₃ units between two layers of CuS₄ tetrahedra.^{46,47} The trilayers are stitched together by sulfur–sulfur covalent bonds. There is an equivalent structure for CuSe, named klockmannite.⁴⁸ On the other hand, no other metal ions are known to crystallize with sulfur (or with selenium) in the same structure, or in any structure that resembles covellite. In a previous work of ours, we evidenced how covellite NCs could easily incorporate Cu⁺ cations, at room temperature, up to a stoichiometry around Cu₂S.⁴² During this incorporation, despite that some XRD reflections of covellite were maintained (albeit with a shift to lower angles), the overall structure underwent partial amorphization. We also demonstrated that the insertion of Cu⁺ ions was charge-compensated by the acquisition of an equimolar amount of electrons, made possible by the oxidation of a fraction of Cu⁺ ions remaining in the solution phase to Cu²⁺. A logical extension of those findings was then to explore whether a similar reaction scheme could work with other metal ions too, and, if so, under what conditions such ions could react with covellite NCs and what would be the products of the reaction. For Hg²⁺ and Cd²⁺ cations studied here, the mechanism operative for the Cu⁺ insertion case discussed above (part of Cu⁺ ions in solution is oxidized to Cu²⁺ and provides electrons to charge-balance the entry of Cu⁺ ions in the NCs) cannot work (Hg and Cd are already at their highest oxidation state). This left room to other various possibilities: (i) the guest ions may be capable of replacing the Cu⁺ ions in the covellite lattice, as in a standard CE reaction, but then the anion framework would have to reorganize considerably; (ii) incorporation of the ions in the NCs would be feasible, provided it could be supported by a source of electrons in the reaction environment; or (iii) a combinations of the two former mechanisms could be operative, for example there could be both incorporation and CE.

Our experiments, reported here, supported a combination of the two mechanisms. First, for both cations tested, when the reactions were performed in the absence of ascorbic acid, limited reactivity was found (we recall that the molar ratio of the guest cations (Cd²⁺ or Hg²⁺) to Cu⁺ ions from covellite CuS, in all the reactions discussed in this work was 1:1, unless otherwise stated). Table 1, second column, lists the M:Cu ratios (M = Cd, Hg) in the CuS NCs as found by elemental analysis (according to ICP-OES) on the samples purified after 24 h of reaction. In all samples, the fraction of cations incorporated in the CuS NCs was low, around 5% for Hg and 1% for Cd. Because of such low amount of cations incorporated, chemical quantification by ICP-OES analysis on a bulk sample of NCs was preferred to EDS analysis, which is instead a local analysis and is performed on groups of NCs in

the electron microscope. The limited reactivity of covellite NCs in the absence of ascorbic acid could be evidenced by the little change in the XRD patterns (which can still be indexed as covellite, see Figure 1a), morphology (Figure S1), and high-resolution XPS (S 2p) (Figure S6b,c) of NCs collected after 24 h of reaction with Cd²⁺ and Hg²⁺ cations without ascorbic acid.

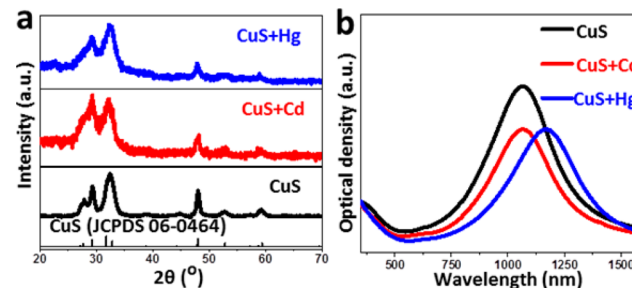


Figure 1. XRD patterns (a) and optical spectra (b) of as-synthesized covellite (CuS) NCs, and NCs collected after mixing CuS with Cd²⁺ (red) and Hg²⁺ (blue) for 24 h, in the absence of ascorbic acid.

Despite the low degree of incorporation of cations (which perhaps in some cases was just a surface adsorption phenomenon), damping and red-shift of the NIR absorption band (the latter due to a localized surface plasmon resonance, LSPR) was seen in the optical absorption spectra of the solutions of NCs at 24 h, with varying degree from cation to cation (Figure 1b). This indicates that the NIR LSPR of covellite NCs is strongly sensitive to various environmental factors. Similarly, djurleite (Cu_{1.94}S) NCs (composition close to Cu₂S) exhibited limited reactivity with Cd²⁺ and Hg²⁺ cations in the absence of reducing agent (Figure S4a, Table S2), except that their weak NIR plasmon absorbance (due to the presence of Cu vacancies) was further damped and red-shifted upon mixing the NCs with cations (Figure S4b).

For reactions of covellite (CuS) carried out in the presence of ascorbic acid, however, much higher M:Cu ratios (M = Cd, Hg) were found in the NCs (see Table 1, third column and Table S1, the latter reporting also the compositions as found by EDS analysis). In contrast, the reactivity of djurleite (Cu_{1.94}S) NCs was not significantly increased by the presence of ascorbic acid for both cations (Figure S4c and Table S2), although the formation of additional Hg₂Br₂, in the Hg case, complicated the XRD analysis: only 7% of Hg and 0.3% of Cd were detected in the resulting NCs after 24 h (Table S2). The higher reactivity of the covellite NCs was also confirmed by XPS analysis of the purified NCs (Figure S6d,e). Here, the spectral features in the S 2p region, which allows discrimination between sulfides and disulfides,⁴² were clearly supporting the almost complete absence of signal from disulfides in the final NCs, which are instead present in the initial covellite NCs due to the S–S covalent bonds in their structure. Therefore, as the vast majority of S–S bonds were broken in the reacted NCs, we expect a significant reorganization of the crystal lattice for the reactions tested. The discussion that follows examines in detail the individual cation cases and reports, unless otherwise stated, the results of reactions on covellite NCs performed in the presence of ascorbic acid.

Reactions with Cd²⁺ ions. Panels a and b of Figure 2 compare low-magnification TEM images of the initial CuS sample and of the same sample after 24 h incubation in a mixture of Cd²⁺ ions and ascorbic acid. The overall size and

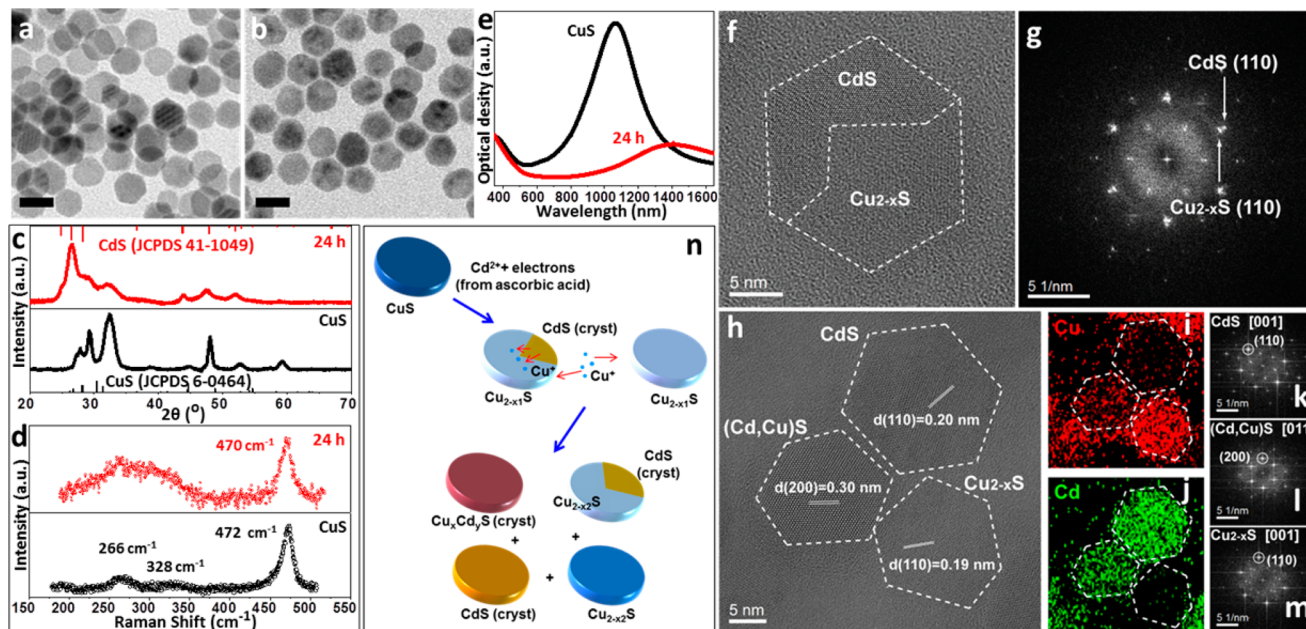


Figure 2. TEM images of the as-synthesized covellite CuS NCs (a) and Cd-incorporated NCs achieved by reacting covellite NCs with Cd²⁺ cations in the presence of ascorbic acid for 24 h (b). The scale bar is 20 nm. XRD patterns (c), Raman spectra (d), and optical spectra (e) of samples shown in a and b. (f) HRTEM image and (g) corresponding FFT of a representative single CdS/Cu_{2-x}S nanoparticle collected at 4 h by reacting the as-synthesized covellite CuS NCs with Cd²⁺ cations in the presence of ascorbic acid. (h) HRTEM image and (i,j) corresponding EDS mapping. (k–m) FFT of the single NPs shown in h. (n) Schematic illustration of the reaction of CuS NCs with Cd²⁺ cations in the presence of ascorbic acid.

shape of the initial sample (and their relative distributions) were essentially preserved. Size-distribution histograms of the initial and the final NCs, as well as TEM images of initial and intermediate samples, are shown in Figures S5a,b and S7a–e, respectively. Experimental XRD patterns of aliquots taken at 1, 2, 4, and 24 h evidenced the emergence of peaks belonging to the CdS phase (Figure S7f). The XRD pattern of the sample at 24 h, reported in Figure 2c (top, to be compared to the pattern of the initial covellite NC, shown in c, bottom), carried strong signatures of CdS, while the assignment of the remaining peaks was less straightforward. HRTEM and EDS analyses of the 4-h (intermediate) and 24-h samples revealed a mixture of NC structures. The predominant types of particles were heterostructures composed of domains that could be indexed as CdS and Cu_{2-x}S ($0 < x < 1$), respectively (Figure 2f,g). In addition, there were entirely exchanged NCs, i.e. CdS nanoplatelets, and platelets with phases possibly matching various Cu_{2-x}S bulk phases, but which, according to EDS analysis, contained a fraction of Cd too (Figure 2h–m). In the 24-h sample even chalcocite Cu₂S NCs were detected. An increasing degree of incorporation of Cd was found in the NCs over reaction time, from 5% (with respect to Cu) at 1 h, to 22% at 24 h, as evidenced by the ICP analyses (see Table 1 and Table S1).

We can hypothesize that the incorporation of Cd²⁺ ions in the covellite NCs, aided by the overall reducing environment, can locally initiate CE, with reorganization of the anion (sulfur) framework and the consequent formation of CdS domains, a process that eventually can spread to the whole NC. The Cu⁺ ions that are released from the CdS-exchanged domains can diffuse to the not exchanged domains within the same NC. This would explain the formation of CdS–Cu_{2-x}S heterostructures, such as the one displayed in Figure 2f. On the other hand, the presence of Cu_{2-x}S platelets can be rationalized by the incorporation of Cu⁺ ions that had been previously released from the exchanged NCs to the solution phase. This is similar

to what was found previously by us⁴² when treating covellite NCs with Cu⁺ ions. These hypotheses were additionally backed by the experimental evidence that elemental analysis (by ICP–OES) of the solution phase revealed no appreciable Cu in the supernatant after NCs precipitated from the solution: therefore, even if Cu⁺ ions were released in solution, they were unstable there and tended to react with the CuS NCs/domains. Partial support to the CuS → Cu_{2-x}S transformation came also from the red-shift and strong damping of the NIR absorbance as the reaction proceeded (Figure 2e, see also Figure S7h). This is in line with our previous work on the evolution of CuS NCs to Cu_{2-x}S,⁴² and is due to the decrease in the density of free carriers in the NCs that accompanies such transformation.

The transformations were also corroborated by Raman analysis (Figure 2d). The Raman spectrum of the pristine CuS NCs exhibited vibration modes at 472 and 266 cm⁻¹ (see also Figure S7g), which are in good agreement with the Raman spectra of CuS reported by Ishii et al. and Peiris et al.^{47,49} The peak at 266 cm⁻¹ corresponds to a Cu–S vibrational mode,⁵⁰ while the intensity of the initially intense peak at 472 cm⁻¹, attributed to a S–S stretching mode, decreased (relative to the peak at around 266 cm⁻¹) as the stoichiometry evolved from CuS to Cu_{2-x}S ($0 < x < 1$). A broad peak around 300–330 cm⁻¹ might be due to the silicon substrate, as its contribution was seen in all the samples analyzed (see Figure S11 for the Raman spectrum from the substrate only). After 24 h reaction with Cd²⁺, a broad feature ranging from 220 to 350 cm⁻¹ emerged, which might be due to the overlapping modes of Cu–S and Cd–S (the longitudinal optical phonon mode of CdS peaks at around 300 cm⁻¹).⁵¹ In comparison, the initial Raman peak at around 472 cm⁻¹ had lost considerable intensity, an indication that part of the copper sulfide phase was transformed to CdS and most likely the remaining part had evolved to a copper sulfide phase richer in Cu than the initial covellite NCs.

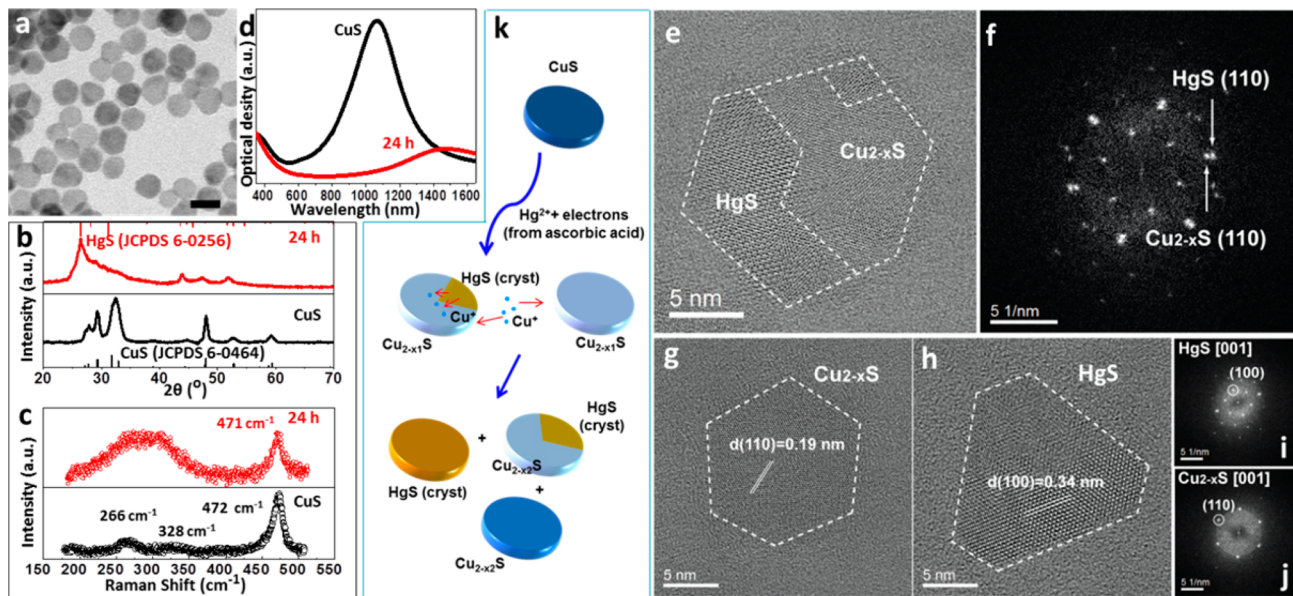


Figure 3. (a) TEM image of NCs collected at 24 h by reacting the covellite CuS NCs with Hg^{2+} cations in the presence of ascorbic acid. The scale bar is 20 nm. (XRD patterns (b), Raman spectra (c), and optical spectra (d) of as-synthesized covellite CuS NCs and Hg-incorporated samples shown in a. (e) HRTEM image and (f) FFT of a representative single $\text{HgS}/\text{Cu}_{2-x}\text{S}$ nanoparticle collected at 4 h by reacting the as-synthesized covellite CuS NCs with Hg^{2+} cations in the presence of ascorbic acid. (g,h) HRTEM images of individual NCs collected at 24 h. (i,j) Corresponding FFT of the single NCs shown in h and g, respectively. (k) Schematic illustration of the reaction of CuS NCs with Hg^{2+} cations in the presence of ascorbic acid.

We also carried out reactions using a large excess of Cd^{2+} ions (with a Cd:Cu feed ratio of 10:1). These experiments produced a sample in which the Cd:Cu:S ratios in the NCs were 0.39:1.1:1, that is, no complete cation exchange could be achieved (see Figure S9c,d). This makes sense, if one considers that the concomitant introduction of Cd^{2+} ions and of electrons (provided by ascorbic acid) in the NCs can proceed as long as there are S–S bonds that can be reduced. The S atoms involved in this bond type represent 66% of the overall number S atoms in covellite, and the rupture of each bond operated by two electrons permits the entry of one Cd^{2+} ion. Therefore, the theoretical limit of incorporation of Cd^{2+} atoms would correspond to 33% of the total number of S and Cu atoms in covellite, which is very close to the ratio found experimentally. Clearly, in this case too, the incorporated Cd ions trigger cation exchange reactions, with release of Cu ions that could diffuse then to the not exchanged domains/NCs. It is noteworthy that even when working with such high Cd:Cu feed ratios (10:1) no Cu could be detected in solution (that is, all Cu^+ ions stayed or were reinserted in the NCs).

Reactions with Hg^{2+} Ions. The reactivity of CuS NCs toward Hg^{2+} cations in the absence of ascorbic acid was limited, although the incorporation of Hg after 24 h could reach 5% (Table 1), higher than that of Cd. On the other hand, in analogy with the case of reaction with Cd^{2+} cations discussed earlier, a more pronounced reactivity with Hg^{2+} was seen in the presence of ascorbic acid. Here again, both size and shape of the NCs were basically preserved (see Figure 3a, Figure S8a–d, and S8c portraying additional images of intermediate samples and the size distribution histogram of the 24 h sample). However, the XRD pattern of the sample after 24 h reaction time (Figure 3b), and those of the intermediate samples (see Figure S8e), evidenced the formation of the HgS phase over time. Other peaks were present, which made the assignment more difficult. These peaks could be due to a mixture of Cu_{2-x}S

phases ($0 < x < 1$), although the diffraction peaks from HgS became predominant over time. In analogy with the reactions involving Cd^{2+} ions, negligible amounts of Cu species were released to the solution, as revealed by elemental analysis (by ICP–OES), and can be interpreted along the same lines as for the reactions with Cd^{2+} . The incorporated amount of Hg was higher here than for the Cd^{2+} case: it ranged from around 10% (relative to Cu) at 1 h, to 20% at 24 h (see Table 1 and Table S1, the latter reporting also compositions as found by EDS analysis). The phase transformation from covellite to Cu_{2-x}S ($0 < x < 1$) and HgS was concomitantly accompanied by a marked red-shift and strong damping of NIR absorption (Figure 3d and Figure S8f). According to HRTEM and EDS analysis, the sample was composed of a mixture of $\text{HgS}/\text{Cu}_{2-x}\text{S}$ heterostructures, often containing more than one HgS domain per NC (Figure 3e,f) and fully exchanged HgS NCs, as well as Cu_{2-x}S NCs (Figure 3g–j), the latter particles this time containing only a minor fraction of Hg. The Raman spectra of the 24-h sample was in line with the results discussed for the Cd^{2+} reaction, that is, with the most notable and interpretable change being the damping of the strong peak initially at 472 cm^{-1} (Figure 3c). Overall, the reaction scheme (Figure 3k) was therefore not much different from that involving the Cd^{2+} ions (Figure 2n).

In the reaction with excess Hg^{2+} cations (with a starting Hg:Cu feed ratio equal to 10:1), the final Hg:Cu:S molar ratios, as measured by ICP, were around 0.6:1:1. The Hg:Cu ratio ($0.6:1 = 0.55:1$) was higher than the theoretical limit set by the fact that the Hg incorporation should stop when all S–S bonds are broken (0.33, see the Cd case discussed earlier). This apparent inconsistency was clarified by XRD analysis (see Figure S9c), according to which this sample contained an important contribution from a CuHgSBr phase.⁵² This is interesting, since this compound is usually synthesized by reacting HgS with CuBr ,⁵² while here it was formed by reacting

CuS with HgBr. This compound is, however, unstable under the electron beam, as by HRTEM we could only unequivocally identify HgS, chalcocite, and covellite-like Cu_{2-x}S NCs (Figure S10). The Hg case, however, will require further scrutiny.

CONCLUSIONS

We have studied the incorporation of heavy metal Cd^{2+} and Hg^{2+} cations in covellite (CuS) NCs at room temperature, in the presence of a mild reducing agent such as ascorbic acid. The incorporation of guest metal cations is promoted by the breaking of the S–S bonds, operated by the reducing agent. A negligible fraction of Cu species could be detected in the solution phase, due to the recapture of released Cu by the not exchanged CuS domains or by the remaining CuS NCs, upon the incorporation of Cd^{2+} and Hg^{2+} cations. This is much different from the previously reported CE studies on various other copper chalcogenide NCs. This notable feature and the mechanism proposed in this study extend the knowledge on nanoscale chemical transformations.

ASSOCIATED CONTENT

Supporting Information

The Supporting Information is available free of charge on the ACS Publications website at DOI: [10.1021/acs.chemmater.5b03892](https://doi.org/10.1021/acs.chemmater.5b03892).

Additional TEM images, size distribution histograms, XPS spectra, XRD patterns, EDS mapping, optical spectra, and elemental analyses (PDF).

AUTHOR INFORMATION

Corresponding Author

*liberato.manna@iit.it.

Notes

The authors declare no competing financial interest.

ACKNOWLEDGMENTS

The research leading to these results has received funding from the European Union's Seventh Framework Programme FP7/2007-2013 under grant agreements 614897 (ERC Grant TRANS-NANO).

REFERENCES

- Zhao, Y.; Pan, H.; Lou, Y.; Qiu, X.; Zhu, J.; Burda, C. Plasmonic Cu_{2-x}S Nanocrystals: Optical and Structural Properties of Copper-Deficient Copper(I) Sulfides. *J. Am. Chem. Soc.* **2009**, *131*, 4253–4261.
- Luther, J. M.; Jain, P. K.; Ewers, T.; Alivisatos, A. P. Localized Surface Plasmon Resonances Arising from Free Carriers in Doped Quantum Dots. *Nat. Mater.* **2011**, *10*, 361–366.
- Dorfs, D.; Härtling, T.; Miszta, K.; Bigall, N. C.; Kim, M. R.; Genovese, A.; Falqui, A.; Povia, M.; Manna, L. Reversible Tunability of the near-Infrared Valence Band Plasmon Resonance in Cu_{2-x}Se Nanocrystals. *J. Am. Chem. Soc.* **2011**, *133*, 11175–11180.
- Hsu, S.-W.; On, K.; Tao, A. R. Localized Surface Plasmon Resonances of Anisotropic Semiconductor Nanocrystals. *J. Am. Chem. Soc.* **2011**, *133*, 19072–19075.
- Hsu, S.-W.; Bryks, W.; Tao, A. R. Effects of Carrier Density and Shape on the Localized Surface Plasmon Resonances of Cu_{2-x}S Nanodisks. *Chem. Mater.* **2012**, *24*, 3765–3771.
- Niezgoda, J. S.; Harrison, M. A.; McBride, J. R.; Rosenthal, S. J. Novel Synthesis of Chalcopyrite $\text{Cu}_x\text{In}_y\text{S}_2$ Quantum Dots with Tunable Localized Surface Plasmon Resonances. *Chem. Mater.* **2012**, *24*, 3294–3298.
- Kriegel, I.; Jiang, C.; Rodríguez-Fernández, J.; Schaller, R. D.; Talapin, D. V.; da Como, E.; Feldmann, J. Tuning the Excitonic and Plasmonic Properties of Copper Chalcogenide Nanocrystals. *J. Am. Chem. Soc.* **2012**, *134*, 1583–1590.
- Liu, X.; Wang, X.; Zhou, B.; Law, W.-C.; Cartwright, A. N.; Swihart, M. T. Size-Controlled Synthesis of Cu_{2-x}E ($\text{E} = \text{S}, \text{Se}$) Nanocrystals with Strong Tunable Near-Infrared Localized Surface Plasmon Resonance and High Conductivity in Thin Films. *Adv. Funct. Mater.* **2013**, *23*, 1256–1264.
- Wei, T.; Liu, Y.; Dong, W.; Zhang, Y.; Huang, C.; Sun, Y.; Chen, X.; Dai, N. Surface-Dependent Localized Surface Plasmon Resonances in CuS Nanodisks. *ACS Appl. Mater. Interfaces* **2013**, *5*, 10473–10477.
- Xie, Y.; Carbone, L.; Nobile, C.; Grillo, V.; D'Agostino, S.; Della Sala, F.; Giannini, C.; Altamura, D.; Oelsner, C.; Kryschi, C.; Cozzoli, P. D. Metallic-Like Stoichiometric Copper Sulfide Nanocrystals: Phase- and Shape-Selective Synthesis, Near-Infrared Surface Plasmon Resonance Properties, and Their Modeling. *ACS Nano* **2013**, *7*, 7352–7369.
- Yang, H.-J.; Chen, C.-Y.; Yuan, F.-W.; Tuan, H.-Y. Designed Synthesis of Solid and Hollow Cu_{2-x}Te Nanocrystals with Tunable Near-Infrared Localized Surface Plasmon Resonance. *J. Phys. Chem. C* **2013**, *117*, 21955–21964.
- Liu, X.; Wang, X.; Swihart, M. T. $\text{Cu}_{2-x}\text{S}_{1-y}\text{Se}_y$ Alloy Nanocrystals with Broadly Tunable Near-Infrared Localized Surface Plasmon Resonance. *Chem. Mater.* **2013**, *25*, 4402–4408.
- Kriegel, I.; Rodríguez-Fernández, J.; Wisnet, A.; Zhang, H.; Waurisch, C.; Eychmüller, A.; Dubavik, A.; Govorov, A. O.; Feldmann, J. Shedding Light on Vacancy-Doped Copper Chalcogenides: Shape-Controlled Synthesis, Optical Properties, and Modeling of Copper Telluride Nanocrystals with Near-Infrared Plasmon Resonances. *ACS Nano* **2013**, *7*, 4367–4377.
- Yang, H.-J.; Chen, C.-Y.; Yuan, F.-W.; Tuan, H.-Y. Designed Synthesis of Solid and Hollow Cu_{2-x}Te Nanocrystals with Tunable Near-Infrared Localized Surface Plasmon Resonance. *J. Phys. Chem. C* **2013**, *117*, 21955–21964.
- Faucheaux, J. A.; Stanton, A. L. D.; Jain, P. K. Plasmon Resonances of Semiconductor Nanocrystals: Physical Principles and New Opportunities. *J. Phys. Chem. Lett.* **2014**, *5*, 976–985.
- Saldanha, P. L.; Brescia, R.; Prato, M.; Li, H.; Povia, M.; Manna, L.; Lesnyak, V. Generalized One-Pot Synthesis of Copper Sulfide, Selenide-Sulfide, and Telluride-Sulfide Nanoparticles. *Chem. Mater.* **2014**, *26*, 1442–1449.
- Balitskii, O. A.; Sytnyk, M.; Stangl, J.; Primetzhofer, D.; Groiss, H.; Heiss, W. Tuning the Localized Surface Plasmon Resonance in Cu_{2-x}Se Nanocrystals by Postsynthetic Ligand Exchange. *ACS Appl. Mater. Interfaces* **2014**, *6*, 17770–17775.
- Lie, S. Q.; Wang, D. M.; Gao, M. X.; Huang, C. Z. Controllable Copper Deficiency in Cu_{2-x}Se Nanocrystals with Tunable Localized Surface Plasmon Resonance and Enhanced Chemiluminescence. *Nanoscale* **2014**, *6*, 10289–10296.
- Wang, X.; Swihart, M. T. Controlling the Size, Shape, Phase, Band Gap, and Localized Surface Plasmon Resonance of Cu_{2-x}S and $\text{Cu}_x\text{In}_y\text{S}$ Nanocrystals. *Chem. Mater.* **2015**, *27*, 1786–1791.
- Liu, M.; Xue, X.; Ghosh, C.; Liu, X.; Liu, Y.; Furlani, E. P.; Swihart, M. T.; Prasad, P. N. Room-Temperature Synthesis of Covellite Nanoplatelets with Broadly Tunable Localized Surface Plasmon Resonance. *Chem. Mater.* **2015**, *27*, 2584–2590.
- Liu, X.; Wang, X.; Swihart, M. T. Composition-Dependent Crystal Phase, Optical Properties, and Self-Assembly of Cu–Sn–S Colloidal Nanocrystals. *Chem. Mater.* **2015**, *27*, 1342–1348.
- Comin, A.; Manna, L. New Materials for Tunable Plasmonic Colloidal Nanocrystals. *Chem. Soc. Rev.* **2014**, *43*, 3957–3975.
- Zhou, M.; Zhang, R.; Huang, M.; Lu, W.; Song, S.; Melancon, M. P.; Tian, M.; Liang, D.; Li, C. A Chelator-Free Multifunctional [^{64}Cu]CuS Nanoparticle Platform for Simultaneous Micro-PET/Ct Imaging and Photothermal Ablation Therapy. *J. Am. Chem. Soc.* **2010**, *132*, 15351–15358.

- (24) Li, Y.; Lu, W.; Huang, Q.; Li, C.; Chen, W. Copper Sulfide Nanoparticles for Photothermal Ablation of Tumor Cells. *Nanomedicine* **2010**, *5*, 1161–1171.
- (25) Hessel, C. M.; Pattani, V. P.; Rasch, M.; Panthani, M. G.; Koo, B.; Tunnell, J. W.; Korgel, B. A. Copper Selenide Nanocrystals for Photothermal Therapy. *Nano Lett.* **2011**, *11*, 2560–2566.
- (26) Tian, Q.; Tang, M.; Sun, Y.; Zou, R.; Chen, Z.; Zhu, M.; Yang, S.; Wang, J.; Wang, J.; Hu, J. Hydrophilic Flower-Like CuS Superstructures as an Efficient 980 nm Laser-Driven Photothermal Agent for Ablation of Cancer Cells. *Adv. Mater.* **2011**, *23*, 3542–3547.
- (27) Tian, Q.; Jiang, F.; Zou, R.; Liu, Q.; Chen, Z.; Zhu, M.; Yang, S.; Wang, J.; Wang, J.; Hu, J. Hydrophilic Cu₉S₅ Nanocrystals: A Photothermal Agent with a 25.7% Heat Conversion Efficiency for Photothermal Ablation of Cancer Cells in Vivo. *ACS Nano* **2011**, *5*, 9761–9771.
- (28) Zhao, Y.; Burda, C. Development of Plasmonic Semiconductor Nanomaterials with Copper Chalcogenides for a Future with Sustainable Energy Materials. *Energy Environ. Sci.* **2012**, *5*, 5564–5576.
- (29) Li, W.; Zamani, R.; Rivera Gil, P.; Pelaz, B.; Ibáñez, M.; Cadavid, D.; Shavel, A.; Alvarez-Puebla, R. A.; Parak, W. J.; Arbiol, J.; Cabot, A. CuTe Nanocrystals: Shape and Size Control, Plasmonic Properties, and Use as Sers Probes and Photothermal Agents. *J. Am. Chem. Soc.* **2013**, *135*, 7098–7101.
- (30) Li, B.; Wang, Q.; Zou, R.; Liu, X.; Xu, K.; Li, W.; Hu, J. Cu_{7.2}S₄ Nanocrystals: A Novel Photothermal Agent with a 56.7% Photothermal Conversion Efficiency for Photothermal Therapy of Cancer Cells. *Nanoscale* **2014**, *6*, 3274–3282.
- (31) Guo, L.; Yan, D. D.; Yang, D.; Li, Y.; Wang, X.; Zalewski, O.; Yan, B.; Lu, W. Combinatorial Photothermal and Immuno Cancer Therapy Using Chitosan-Coated Hollow Copper Sulfide Nanoparticles. *ACS Nano* **2014**, *8*, 5670–5681.
- (32) Wang, S.; Riedinger, A.; Li, H.; Fu, C.; Liu, H.; Li, L.; Liu, T.; Tan, L.; Barthel, M. J.; Pugliese, G.; De Donato, F.; Scotto D'Abusco, M.; Meng, X.; Manna, L.; Meng, H.; Pellegrino, T. Plasmonic Copper Sulfide Nanocrystals Exhibiting near-Infrared Photothermal and Photodynamic Therapeutic Effects. *ACS Nano* **2015**, *9*, 1788–1800.
- (33) Casavola, M.; van Huis, M. A.; Bals, S.; Lambert, K.; Hens, Z.; Vanmaekelbergh, D. Anisotropic Cation Exchange in PbSe/CdSe Core/Shell Nanocrystals of Different Geometry. *Chem. Mater.* **2012**, *24*, 294–302.
- (34) Jain, P. K.; Amirav, L.; Aloni, S.; Alivisatos, A. P. Nano-heterostructure Cation Exchange: Anionic Framework Conservation. *J. Am. Chem. Soc.* **2010**, *132*, 9997–9999.
- (35) Sadtler, B.; Demchenko, D. O.; Zheng, H.; Hughes, S. M.; Merkle, M. G.; Dahmen, U.; Wang, L.-W.; Alivisatos, A. P. Selective Facet Reactivity During Cation Exchange in Cadmium Sulfide Nanorods. *J. Am. Chem. Soc.* **2009**, *131*, 5285–5293.
- (36) Robinson, R. D.; Sadtler, B.; Demchenko, D. O.; Erdonmez, C. K.; Wang, L.-W.; Alivisatos, A. P. Spontaneous Superlattice Formation in Nanorods through Partial Cation Exchange. *Science* **2007**, *317*, 355–358.
- (37) Son, D. H.; Hughes, S. M.; Yin, Y.; Paul Alivisatos, A. Cation Exchange Reactions in Ionic Nanocrystals. *Science* **2004**, *306*, 1009–1012.
- (38) Jeong, U.; Kim, J.-U.; Xia, Y.; Li, Z.-Y. Monodispersed Spherical Colloids of Se@CdSe: Synthesis and Use as Building Blocks in Fabricating Photonic Crystals. *Nano Lett.* **2005**, *5*, 937–942.
- (39) Wark, S. E.; Hsia, C.-H.; Son, D. H. Effects of Ion Solvation and Volume Change of Reaction on the Equilibrium and Morphology in Cation-Exchange Reaction of Nanocrystals. *J. Am. Chem. Soc.* **2008**, *130*, 9550–9555.
- (40) Luther, J. M.; Zheng, H.; Sadtler, B.; Alivisatos, A. P. Synthesis of PbS Nanorods and Other Ionic Nanocrystals of Complex Morphology by Sequential Cation Exchange Reactions. *J. Am. Chem. Soc.* **2009**, *131*, 16851–16857.
- (41) De Trizio, L.; Li, H.; Casu, A.; Genovese, A.; Sathya, A.; Messina, G. C.; Manna, L. Sn Cation Valency Dependence in Cation Exchange Reactions Involving Cu_{2-x}Se Nanocrystals. *J. Am. Chem. Soc.* **2014**, *136*, 16277–16284.
- (42) Xie, Y.; Riedinger, A.; Prato, M.; Casu, A.; Genovese, A.; Guardia, P.; Sottini, S.; Sangregorio, C.; Miszta, K.; Ghosh, S.; Pellegrino, T.; Manna, L. Copper Sulfide Nanocrystals with Tunable Composition by Reduction of Covellite Nanocrystals with Cu⁺ Ions. *J. Am. Chem. Soc.* **2013**, *135*, 17630–17637.
- (43) Smith, A. M.; Nie, S. Bright and Compact Alloyed Quantum Dots with Broadly Tunable near-Infrared Absorption and Fluorescence Spectra through Mercury Cation Exchange. *J. Am. Chem. Soc.* **2011**, *133*, 24–26.
- (44) Li, H.; Brescia, R.; Povia, M.; Prato, M.; Bertoni, G.; Manna, L.; Moreels, I. Synthesis of Uniform Disk-Shaped Copper Telluride Nanocrystals and Cation Exchange to Cadmium Telluride Quantum Disks with Stable Red Emission. *J. Am. Chem. Soc.* **2013**, *135*, 12270–12278.
- (45) Gupta, S.; Kershaw, S. V.; Rogach, A. L. 25th Anniversary Article: Ion Exchange in Colloidal Nanocrystals. *Adv. Mater.* **2013**, *25*, 6923–6944.
- (46) Gainov, R. R.; Dooglav, A. V.; Pen'kov, I. N.; Mukhamedshin, I. R.; Mozgovaya, N. N.; Evlampiev, I. A.; Bryzgalov, I. A. Phase Transition and Anomalous Electronic Behavior in the Layered Superconductor CuS Probed by Nqr. *Phys. Rev. B: Condens. Matter Mater. Phys.* **2009**, *79*, 075115.
- (47) Peiris, S. M.; Sweeney, J. S.; Campbell, A. J.; Heinz, D. L. Pressure-Induced Amorphization of Covellite, CuS. *J. Chem. Phys.* **1996**, *104*, 11–16.
- (48) Milman, V. Klockmannite, CuSe: Structure, Properties and Phase Stability from Ab Initio Modeling. *Acta Crystallogr., Sect. B: Struct. Sci.* **2002**, *58*, 437–447.
- (49) Ishii, M.; Shibata, K.; Nozaki, H. Anion Distributions and Phase Transitions in CuS_{1-x}Se_x (X = 0–1) Studied by Raman Spectroscopy. *J. Solid State Chem.* **1993**, *105*, 504–511.
- (50) Kumar, P.; Nagarajan, R. An Elegant Room Temperature Procedure for the Precise Control of Composition in the Cu–S System. *Inorg. Chem.* **2011**, *50*, 9204–9206.
- (51) Schreder, B.; Dem, C.; Schmitt, M.; Materny, A.; Kiefer, W.; Winkler, U.; Umbach, E. Raman Spectroscopy of II–VI Semiconductor Nanostructures: Cds Quantum Dots. *J. Raman Spectrosc.* **2003**, *34*, 100–103.
- (52) Moro'oka, M.; Ohki, H.; Yamada, K.; Okuda, T. Crystal Structure of High Temperature Phase and Ionic Conductivity Mechanism of CuHgSX (X = Cl, Br). *Bull. Chem. Soc. Jpn.* **2003**, *76*, 2111–2115.